A PERFORMANCE ANALYSIS FOR MULTI-RIS-ASSISTED FULL DUPLEX WIRELESS COMMUNICATION SYSTEM

Farjam Karim, Bishmita Hazarika, Sandeep Kumar Singh, and Keshav Singh

Institute of Communications Engineering, National Sun Yat-sen University, Kaohsiung, Taiwan
Email: {farjamkarim, me.bishmita}@gmail.com, {sks, keshav.singh}@mail.nsysu.edu.tw

ABSTRACT

Reconfigurable Intelligent Surface (RIS) is a transformative technology which can enhance the performance of the ubiquitous wireless networks and achieve better signal quality with the aide of multiple reflecting surfaces. In this work, an analytical framework of a RIS-aided full duplex (FD) communication network consisting of a FD-access point (AP) that communicates with an uplink and a downlink users simultaneously is provided. In particular, we analyze the performance of the considered system by deriving analytical expressions of outage probability for both uplink and downlink transmissions. Further, the accuracy of the derived expressions is validated using simulation results. Finally, from the comparative analysis, it is shown that the RIS outperforms the system without RIS providing remarkable improvement in the outage probability.

***Index Terms*—** Reconfigurable intelligent surface (RIS), full duplex (FD), outage probability, uplink, downlink.

1. INTRODUCTION

Over the past few decades use of wireless devices have escalated prominently, yielding its way to a society with inflated demand for impeccable wireless coverage, ubiquitous connectivity and high data speed. To cope up with the demands, it has become crucial to take suitable measures to accommodate the needs for all the connected devices which is exponentially increasing with time. Hence, researchers have started to emphasize on exploring novel and advanced technology alternatives to assist beyond fifth generation (B5G) wireless networks [1]. In this context, reconfigurable intelligent surface (RIS) assisted full duplex has come off as a reasonable research interest since it is one of most probable technology that provides an efficient alternate to the conventional relaying by using a discrete set of meta material reflecting surfaces to assist the communication between wireless devices such as cellular users (CUs), access point (AP), etc. The primary reason of its increasing popularity among the researchers is because of its ability to improve the signal quality with very low power consumption and thereby providing better achievable diversity, higher data rate and more reliable system [2,3]. Furthermore, full duplex (FD) has also marked its way to become a prominent research interest due to its potential to improve the spectral efficiency of the system by transmitting and receiving the signal simultaneously using same resources [4, 5]. RIS is an emerging technology which can have a very high-impact on the performance of communication systems [6]. Hence, the integration of RIS in FD communication system has been well motivated by the researchers [7–9] in order to achieve low power and better reliable RIS-assisted transmission and for having efficient use of the available resources. The authors in [9] have presented a clear demonstration of difference in the achievable rate of the FD and half-duplex (HD) systems.

Besides the above research using single RIS, use of multiple RIS in wireless communication have also been well motivated by researchers in [10–12]. For instance, the authors in [10] used multiple-RIS in a device to device (D2D) FD system and derived the closed form expression of outage probability to analyze its performance. Likewise, in [12] the authors analyzed the performance of multiple-RIS-aided downlink cellular system where average signal to interference and noise ratio (SINR) was maximized by optimizing passive beamforming at each RIS. However, no relevant research on analyzing the performance of multiple RIS considering a more practical and simultaneous uplink and downlink transmission scenario in a muti-user cellular communication system has been done so far. Hence, due to the lack of adequate material in literature, the use and performance of RIS in such systems are yet to be explored and utilized up to their full potential. Therefore, in this paper, the impact of RIS in FD cellular communication system is examined and an analytical framework of a RIS-aided FD communication network consisting of a FD-access point (AP) that communicates with an uplink and a downlink users simultaneously is accommodated. Additionally, the system performance is also analyzed by deriving analytical expressions of outage probability for both uplink and downlink and the accuracy of the expression is derived using simulation and numerical results are validated. Finally, through comparative analysis, it is shown that the RIS outperforms the conventional communication system with no-RIS, providing remarkable improvement in the outage probability at each CU.

Organization: The flow of this paper is organized as follows. Section 2 provides the detailed explanation of the considered system model. In Section 3 analytical expressions of outage probabilities has been derived. Simulation results are discussed in Section 4 and finally, the conclusions are drawn in Section 5.

Notations: Matrix, vector and scalar are denoted by boldface upper case, boldface lower case and lower case letters, respectively. Also, $\mathcal{CN} \sim (0, \sigma^2)$ denotes complex Gaussian distribution with zero mean and variance σ^2. $f_Z(z)$ denotes the probability distribution function (PDF) of the random variable Z. $K.(\cdot)$ represents the modified Bessel function. $(\cdot)^{\mathrm{H}}$ provides the Hermitian of a matrix or vector.

This work was supported by the Ministry of Science and Technology of Taiwan under grants MOST 110-2221-E- 110-020 and MOST 110-2224-E-110 -001.

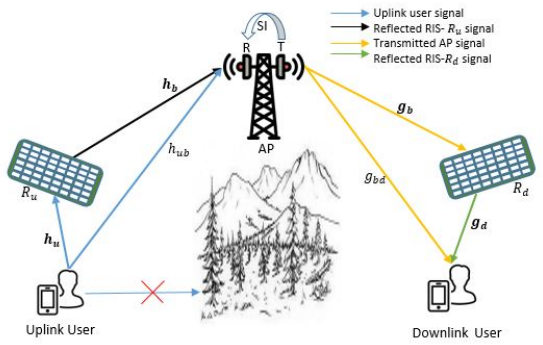

Fig. 1: RIS-aided UL and DL Communication system

2. SYSTEM MODEL

This work considers a FD uplink and downlink communication system, as illustrated in Fig. 1, which comprises of an AP, two RIS, an uplink-CU (UCU) and a downlink-CU (DCU). The AP operates in FD-mode using a single transmit and single receive antenna to communicates with DCU and UCU simultaneously. Both the CUs are implanted with a single antenna and operates in HD mode. In addition to this, UCU uplinks the information to the AP with the aide of RIS (R_u) having K reflecting elements ($\mathcal{K} \in \{1, 2, \cdots, K\}$) and at the same time the AP downlinks another information to DCU using RIS (R_d) having N reflecting elements ($\mathcal{N} \in \{1, 2, \cdots, N\}$).

In the uplink, h_{ub} represents the channel gain of the direct path between UCU and AP. Also, the channel gain between UCU and k^{th} element of R_u is denoted by h_{uk} and h_{kb} depicts the gain between k^{th} element to AP with $k \in \mathcal{K}$. Further, $\theta_k \in [0, 2\pi]$ denotes the phase shift of the k^{th} element of R_u. Correspondingly, in the downlink, the channel gain between AP and n^{th} element of R_d is denoted by g_{bn} whereas g_{nd} represents the channel gain between n^{th} element of R_d and DCU with $n \in \mathcal{N}$. g_{bd} depicts the channel coefficient for direct path between AP and DCU and $\theta_n \in [0, 2\pi]$ denotes the phase shift of the n^{th} element of R_d. Due to non-line of sight (nLoS) nature of direct link between AP and CUs, we assume h_{ub} and g_{bd} follow Rayleigh fading [13] with zero mean and unity variance having probability density function (PDF) given by

$$f_Y(y) = ye^{-y^2/2}. \tag{1}$$

However, due to LoS nature of the links between RIS and all devices, we assume h_{uk}, h_{kb}, g_{bn} and g_{nd} follow Nakagami-m fading [14–16] with PDF given by

$$f_X(x) = \frac{2m^m}{\Gamma(m)\Omega^m} x^{2m-1} \exp\left(-\frac{m}{\Omega}x^2\right), \tag{2}$$

where $X \in \{h_{uk}, h_{kb}, g_{bn}, g_{nd}\}$, and m and Ω are the shape and spread constraints of variable X. Also, without loss of generality, all the channels are assumed to be to be independent and identically distributed.

The UCU uplinks the unit energy information s_u to the AP using transmit power P_u and the corresponding signal received at the AP is given by

$$y_u = \underbrace{(\mathbf{h}_b^{\mathrm{H}}\mathbf{\Theta}\mathbf{h}_u + h_{ub})\sqrt{P_u}s_u}_{\text{desired signal}} + \underbrace{g_{bb}\sqrt{P_b}s_d}_{\text{self interference}} + \underbrace{n_b}_{\text{AWGN}}. \tag{3}$$

where $\mathbf{h}_b = [h_{1b}, h_{2b}, \cdots, h_{Kb}]^{\mathrm{H}}$, $\mathbf{\Theta} = \mathrm{diag}[e^{j\theta_1}, \cdots, e^{j\theta_K}]$, $\mathbf{h}_u = [h_{u1}, h_{u2}, \cdots, h_{uK}]^{\mathrm{H}}$ and $n_b \sim \mathcal{CN}(0, \sigma^2)$ denotes the additive white Gaussian noise (AWGN). g_{bb} denotes the self interference (SI) channel and s_d is the transmit information from AP to DCU with power P_b. The signal to interference and noise ratio (SINR) to decode s_u from y_u at AP can be expressed as

$$\gamma_u = \frac{|\mathbf{h}_b^{\mathrm{H}}\mathbf{\Theta}\mathbf{h}_u + h_{ub}|^2 P_u}{\sigma^2 + P_{SI}}. \tag{4}$$

where P_{SI} is the power of the residual SI[1]. Further, as mentioned earlier, AP is operating in FD mode, therefore, alongwith receiving signal from UCU, AP also transmits information s_d to DCU with a transmit power of P_b. The signal received at DCU can be expressed as

$$y_d = \underbrace{\mathbf{g}_d^{\mathrm{H}}\mathbf{\Phi}\mathbf{g}_b\sqrt{P_b}s_d + g_{bd}\sqrt{P_b}s_d}_{\text{desired signal}} + \underbrace{n_d}_{\text{AWGN}}, \tag{5}$$

where $\mathbf{g}_d = [g_{1d}, g_{2d}, \cdots, g_{Nd}]^{\mathrm{H}}$, $\mathbf{\Phi} = \mathrm{diag}[e^{j\phi_1}, \cdots, e^{j\phi_N}]$, $\mathbf{g}_b = [g_{b1}, g_{b2}, \cdots, g_{bn}]^{\mathrm{H}}$ and $n_d \sim \mathcal{CN}(0,\sigma^2)$ is the AWGN[2]. The signal to noise ratio (SNR) required at DCU for decoding unit energy symbol s_d from y_d is given by

$$\gamma_d = |\mathbf{g}_d^{\mathrm{H}}\mathbf{\Phi}\mathbf{g}_b + g_{bd}|^2 P_b/\sigma^2. \tag{6}$$

3. OUTAGE PROBABILITY

In this section, we investigate the performance of the considered system and derive closed-form expressions of the outage probability at the AP and DCU during uplink and downlink transmission, respectively. As discussed earlier, the UCU uplinks the information to the AP with an SINR, γ_u, given by (4). We derive the PDF of γ_u in the following Lemma:

Lemma 1. *The PDF of SINR γ_u is evaluated as*

$$f_{\gamma_u}(\gamma) = \frac{e^{\frac{-a^2}{2\sigma_{h_r}^2} - \frac{v^2}{4q^2}}}{2q\sqrt{2\pi\sigma_{h_r}^2\gamma\alpha}}\left[\Gamma\left(1, \frac{v^2}{4q}\right) - \Gamma\left(1, q\left(\sqrt{\gamma\alpha} - \frac{v}{2q}\right)^2\right)\right.$$
$$\left. + \frac{v}{2\sqrt{q}}\left(\Gamma\left(\frac{1}{2}, \frac{v^2}{4q}\right) - \Gamma\left(\frac{1}{2}, q\left(\sqrt{\gamma\alpha} - \frac{v}{2q}\right)^2\right)\right)\right], \tag{7}$$

where $\mu_{h_r} = K\left(\frac{\Omega_1\Omega_2}{m_1 m_2}\right)^{\frac{1}{2}} \frac{\Gamma(m_1+0.5)\Gamma(m_2+0.5)}{\Gamma(m_1)\Gamma(m_2)}$, $\sigma_{h_r}^2 = K\Omega_1\Omega_2 - \frac{\mu_{h_r}^2}{K}$, $a = \gamma\alpha - \mu_{h_r}$, $q = \frac{1+\sigma_{h_r}^2}{2\sigma_{h_r}^2}$, $v = \frac{a}{\sigma_{h_r}^2}$ *and* $\alpha = \frac{(|P_{SI}|^2 + \sigma^2)}{P_u}$. *$m_1$ and Ω_1 are the shape and spread parameter of $h_{uk}, \forall k \in \mathcal{K}$, m_2 and Ω_2 are the shape and spread parameter of $h_{kb}, \forall k \in \mathcal{K}$.*

Proof. From (4), we can write

$$\gamma_u = \left|\sum_{k\in\mathcal{K}} |h_{uk}||h_{kb}|e^{-j(\theta_{uk}+\theta_{kb}-\theta_k)} + h_{ub}\right|^2 P_u/(\sigma^2 + P_{SI}), \tag{8}$$

[1]A significant amount of SI can be eliminated using some standard methods like analog and digital self interference cancellation techniques [17, 18]. Therefore, residual SI power is very low as compared to received signal.

[2]Co-channel Interference (CCI) is negligible because of the blocked path between UCU and DCU.

where θ_{uk} and θ_{kb} denoted the angle h_{uk} and h_{kb} respectively. Now, as evident from [19, 20], the SINR is maximized at $(\theta_{uk} + \theta_{kb} = \theta_k)$. Therefore, we also evaluate the PDF considering $(\theta_{uk} + \theta_{kb} = \theta_k) \forall k \in \mathcal{K}$. Next, we assume $h_k \triangleq |h_{uk}||h_{kb}|$. Thus, from (2), we evaluate the PDF of h_k as

$$f_{h_k}(z) = \int_0^\infty \frac{2m_1^{m_1} y^{2m_1-1}}{\Gamma(m_1)\Omega_1^{m_1}} \exp\left(-\frac{m_1}{\Omega_1} y^2\right) \times \frac{2m_2^{m_2} (z/y)^{2m_2-1}}{\Gamma(m_2)\Omega_2^{m_2}} \exp\left(-\frac{m_2}{\Omega_2}(z/y)^2\right) \frac{1}{y} dy \quad (9)$$

Using approach similar to [10], we solve (9) to have

$$f_{h_k}(z) = S_1 z^{m_1+m_2-1} K_{m_1-m_2}\left(2z\sqrt{\frac{m_1 m_2}{\Omega_1\Omega_2}}\right) \quad (10)$$

where $S_1 = \frac{4{m_1}^{m_1} {m_2}^{m_2}}{\Gamma(m_1)\Gamma(m_2)\Omega_1^{m_1}\Omega_2^{m_2}} \left(\frac{m_2\Omega_1}{m_1\Omega_2}\right)^{\frac{m_2-m_1}{2}}$. Using (10) and central limit theorem (CLT), the PDF of $h_r \triangleq \sum_{k=1}^{K} h_k$ can be closely approximated as Gaussian distribution with mean μ_{h_r} and variance $\sigma^2_{h_r}$, and PDF is given by

$$f_{h_r}(y) = \frac{1}{\sigma_{h_r}\sqrt{2\pi}} \exp\left(-(y-\mu_{h_r})^2/2\sigma^2_{h_r}\right) \quad (11)$$

Next, assuming $Z = |h_r + h_{ub}|$, and using (1) and(11), we have the PDF of Z as

$$f_Z(z) = \int_0^z \frac{y}{\sqrt{2\pi\sigma^2_{h_r}}} \exp\left(\frac{-(z-y-\mu_{h_r})^2}{2\sigma^2_{h_r}} - \frac{y^2}{2}\right) dy \quad (12)$$

After some mathematical simplification, we have

$$f_Z(z) = \frac{1}{\sqrt{2\pi\sigma^2_{h_r}}} e^{\frac{-a^2}{2\sigma^2_{h_r}}} \int_0^z y e^{\left(-qy^2+vy\right)} dy \quad (13)$$

Solving (13) using [21, 3.326.4], we obtain PDF of Z as

$$f_Z(z) = \frac{e^{\frac{-a^2}{2\sigma^2_{h_r}} - \frac{v^2}{4q^2}}}{\sqrt{2\pi\sigma^2_{h_r}}} \left[\frac{\Gamma\left(1, \frac{v^2}{4q}\right) - \Gamma\left(1, q\left(z - \frac{v}{2q}\right)^2\right)}{2q} + \frac{v}{2q} \frac{\Gamma\left(\frac{1}{2}, q\left(-\frac{v}{2q}\right)^2 - \Gamma\left(\frac{1}{2}, q\left(z-\frac{v}{2q}\right)^2\right)\right)}{2q^{\frac{1}{2}}}\right] \quad (14)$$

Using PDF of Z, we can express the PDF of Z^2 as

$$f_{(Z^2)}(z) = \frac{e^{\frac{-a^2}{2\sigma^2_{h_r}} - \frac{v^2}{4q^2}}}{\sqrt{2\pi\sigma^2_{h_r}}} \left[\frac{\Gamma\left(1, \frac{v^2}{4q}\right) - \Gamma\left(1, q\left(\sqrt{z} - \frac{v}{2q}\right)^2\right)}{2q} + \frac{v}{2q} \frac{\Gamma\left(\frac{1}{2}, q\left(-\frac{v}{2q}\right)^2\right) - \Gamma\left(\frac{1}{2}, q\left(\sqrt{z}-\frac{v}{2q}\right)^2\right)}{2q^{\frac{1}{2}}}\right] \frac{1}{\sqrt{z}}. \quad (15)$$

Using (8) and (15), we obtain (7). ■

It is evident from (4), that if γ_u fails to cross a minimum target threshold then the uplink will be in outage with the probability of

$$\mathrm{P_{Ou}} = \Pr(\gamma_u < \gamma^1_{th}) = \int_0^{\gamma^1_{th}} f_{\gamma_u}(\gamma) d\gamma. \quad (16)$$

where $\gamma^1_{th} = 2^{r_u} - 1$ with a target rate of r_u.

Theorem 1. *The outage probability at AP during uplink transmission can be expressed as*

$$\mathrm{P_{Ou}} = \int_0^{\gamma^1_{th}} \frac{e^{\frac{-a^2}{2\sigma^2_{h_r}} - \frac{v^2}{4q^2}}}{2q\sqrt{2\pi\sigma^2_{h_r}\gamma\alpha}} \left[\Gamma\left(1, \frac{v^2}{4q}\right) - \Gamma\left(1, q\left(\sqrt{\gamma\alpha} - \frac{v}{2q}\right)^2\right) + \frac{v}{2\sqrt{q}}\left(\Gamma\left(\frac{1}{2}, \frac{v^2}{4q}\right) - \Gamma\left(\frac{1}{2}, q\left(\sqrt{\gamma\alpha} - \frac{v}{2q}\right)^2\right)\right)\right] d\gamma. \quad (17)$$

Proof. The outage probability at AP is obtained by solving (16) using (7). Detailed proof is omitted due to paucity of space. ■

Further, similar to γ_u, the PDF of γ_d is derived in following Lemma:

Lemma 2. *The PDF of SNR γ_d is evaluated using steps similar to* (7) *and obtained as*

$$f_{\gamma_d}(\gamma) = \frac{e^{\frac{-p^2}{2\sigma^2_{g_r}} - \frac{w^2}{4t^2}}}{2t\sqrt{2\pi\sigma^2_{g_r}\gamma\beta}} \left[\Gamma\left(1, \frac{w^2}{4t}\right) - \Gamma\left(1, t\left(\sqrt{\gamma\beta} - \frac{w}{2t}\right)^2\right) + \frac{w}{2\sqrt{t}}\left(\Gamma\left(\frac{1}{2}, \frac{w^2}{4t}\right) - \Gamma\left(\frac{1}{2}, t\left(\sqrt{\gamma\beta} - \frac{w}{2t}\right)^2\right)\right)\right], \quad (18)$$

where $\mu_{g_r} = N\left(\frac{\Omega_3\Omega_4}{m_3 m_4}\right)^{\frac{1}{2}} \frac{\Gamma(m_3+0.5)\Gamma(m_4+0.5)}{\Gamma(m_3)\Gamma(m_4)}$, $\sigma^2_{g_r} = N\Omega_3\Omega_4 - \frac{\mu^2_{g_r}}{N}$, $p = \gamma\beta - \mu_{g_r}$, $t = \frac{1+\sigma^2_{g_r}}{2\sigma^2_{g_r}}$, $w = \frac{p}{\sigma^2_{g_r}}$, *and* $\beta = \sigma^2/P_b$. m_3 *and* Ω_3 *are the shape and spread parameter of* $h_{bn} \forall n \in \mathcal{N}$, m_4 *and* Ω_4 *are the shape and spread parameter of* $h_{nd} \forall n \in \mathcal{N}$.

Furthermore, it is evident from (6), that if γ_d fails to cross a minimum target threshold then the downlink will be in outage with the probability of

$$\mathrm{P_{Od}} = \Pr(\gamma_d < \gamma^2_{th}) = \int_0^{\gamma^2_{th}} f_{\gamma_d}(\gamma) d\gamma. \quad (19)$$

where $\gamma^2_{th} = 2^{r_d} - 1$ with a target rate of r_d.

Theorem 2. *The outage probability at DCU during downlink transmission can be expressed as*

$$\mathrm{P_{Od}} = \int_0^{\gamma^2_{th}} \frac{e^{\frac{-p^2}{2\sigma^2_{g_r}} - \frac{w^2}{4t^2}}}{2t\sqrt{2\pi\sigma^2_{g_r}\gamma\beta}} \left[\Gamma\left(1, \frac{w^2}{4t}\right) - \Gamma\left(1, t\left(\sqrt{\gamma\beta} - \frac{w}{2t}\right)^2\right) + \frac{w}{2\sqrt{t}}\left(\Gamma\left(\frac{1}{2}, \frac{w^2}{4t}\right) - \Gamma\left(\frac{1}{2}, t\left(\sqrt{\gamma\beta} - \frac{w}{2t}\right)^2\right)\right)\right] d\gamma. \quad (20)$$

Proof. The outage probability at DCU is obtained by solving (19) using (18). Detailed proof is omitted due to paucity of space. ■

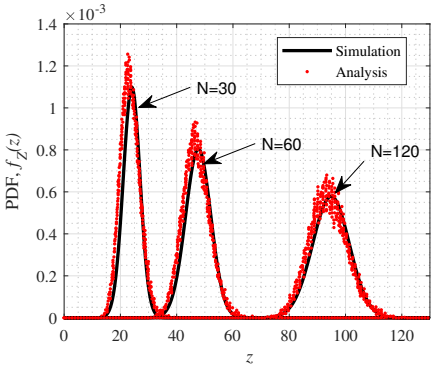

Fig. 2: Joint density Function

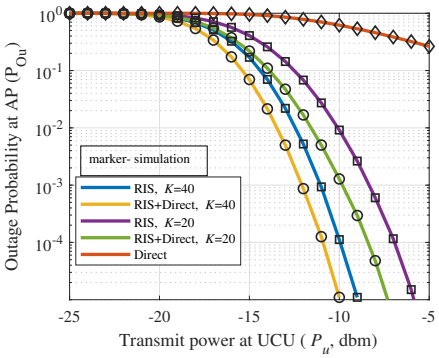

Fig. 3: Outage probability at AP vs uplink power

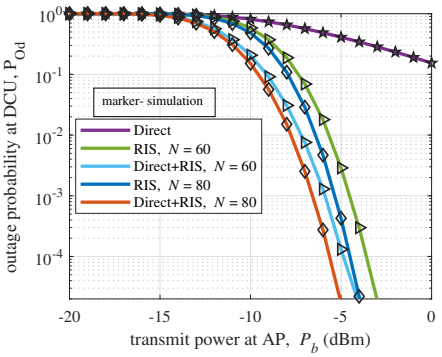

Fig. 4: Outage probability at AP vs downlink power

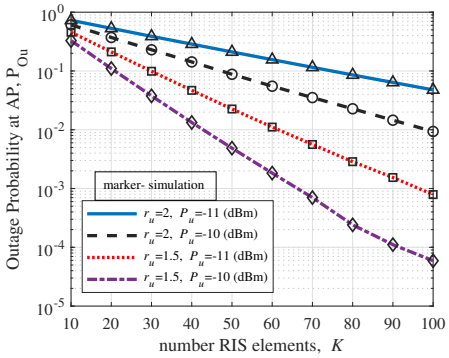

Fig. 5: Outage probability at AP vs number of RIS elements

4. RESULTS AND DISCUSSIONS

In this section, the effectiveness of RIS and the performance of the entire system has been validated with the derived analytical expressions. Unless stated otherwise, $r_u = 1$, $r_d = 1$, $P_{SI} = -10$dB, $\sigma^2 = -90$dBm, $m = 2$, $\Omega = 1$, distance between UCU-R_u = 3m, R_u-AP = 50m, UCU-AP = 50m, AP-R_d = 55m, R_u-DCU= 5m, AP-DCU = 50m respectively. Note that for simulations, we have considered the distance dependent pathloss given by ζ/D^τ where ζ is the reference pathloss with $\zeta = -30$dB for every link and D is used to denote the distance between transmitter and receiver nodes. τ is the pathloss exponent set as $\tau = 3.8$ for the direct path (i.e. UCU-AP and AP-DCU) while we set $\tau = 2.5$ for the following links: UCU-R_u, R_u-AP, AP-R_d, and R_u-DCU [22].

Fig. 2 compares the accuracy of the derived PDF in (12) of the variable $Z = |h_r + h_{ub}|$ with that of the its PDF obtained using simulation. It can be seen that analytical and simulated PDFs follows approximately similar distributions, hence validating the approximation used to obtain (14). Further, it can also be observed that the similarity is more at higher values of N as compared to lower values of N. The reason to this behavior is the CLT approximation considered in (11) which becomes more accurate as the number of elements N increases.

Fig. 3, exhibits the outage probability plotted against the total transmit power available at UCU. It compares the outage probability at AP during uplink transmission considering three different scenario: 1) direct path without RIS, 2) RIS with negligible direct path gain and 3) RIS with considerable direct path gain. The close proximity between analytical and simulated graphs proves the accuracy of the derived expression of outage probability in (17). It can be seen that, due to increase in SINR, the outage probability decreases with an increase in transmit power at UCU. Further, as evident from the figure, outage probability for RIS with negligible direct path gain is lower than the outage probability for direct path gain without RIS. Therefore, use of RIS enhances the performance of the considered system as compared to without-RIS case. It can also observed that the outage probability is further reduced when RIS with considerable direct path gain is considered.

Fig. 4 depicts the plot of outage probability at DCU during the downlink transmission w.r.t. available transmit power at AP obtained for all the three cases discussed in previous figure. As expected, the close proximity between analytical and simulated graphs proves the accuracy of the derived expression of outage probability in (20). Also, similar to previous figure, outage probability decreases with the increase in transmit power at AP and outage probability for RIS with negligible direct path gain is better than that for direct path gain without RIS. Additionally, the outage probability is further enhanced when RIS with considerable direct path gain is considered.

Furthermore, to highlight the impact of number of RIS elements in the outage behavior, we plot outage performance at AP during uplink transmission versus number of RIS elements K at R_u. It is obtained for different values of transmit power P_u available at UCU and target rate at AP. As can be observed, due to the increase in diversity, the outage probability improves with the increase in K. However, because of increase in SINR threshold, the outage probability degrades with increase in target rate at AP. Note that the outage probability at DCU also follows same behavior w.r.t. N at R_d. Thus, depending on the QoSs and available power, one can always choose appropriate number of elements at each RIS. Therefore, in order to obtain enhanced performance, it is suggestible to use multiple RISs in scenarios similar to the proposed one, which is also evident from Fig 3-Fig 5.

5. CONCLUSION

In this paper, an analytical framework of a RIS-aided full duplex (FD) communication network consisting of a FD-access point (AP) that communicates with an uplink and a downlink users simultaneously is presented that can act as a effectual promptuary for more advanced subsequent future researches. We also analyzed the performance of the considered system by deriving analytical expressions of outage probability for both uplink and downlink and validated their accuracy using simulation and numerical results. Finally, through comparative analysis, we have highlighted the importance of RIS as compared to conventional system without RIS.

6. REFERENCES

[1] Y. Liu, X. Wang, G. Boudreau, A. B. Sediq, and H. Abou-Zeid, "A multi-dimensional intelligent multiple access technique for 5G beyond and 6G wireless networks," *IEEE Trans. Wireless Commun.*, vol. 20, no. 2, pp. 1308–1320, Oct. 2021.

[2] Q. Wu and R. Zhang, "Intelligent reflecting surface enhanced wireless network: Joint active and passive beamforming design," in *Proc. IEEE GLOBECOM*, Abu Dhabi, UAE, Feb. 2018, pp. 1–6.

[3] H. Zhang, H. Zhang, B. Di, K. Bian, Z. Han, and L. Song, "Towards ubiquitous positioning by leveraging reconfigurable intelligent surface," *IEEE Commun. Lett.*, vol. 25, no. 1, pp. 284–288, Sep. 2020.

[4] M. H. N. Shaikh, V. A. Bohara, and A. Srivastava, "Performance analysis of a full-duplex MIMO decode-and-forward relay system with self-energy recycling," *IEEE Access*, vol. 8, pp. 226 248–226 266, Dec. 2020.

[5] P. Raut, K. Singh, W. Huang, C. Li, and M. Alouini, "Reliability analysis of FD-enabled multi-UAV systems with short-packet communication," *IEEE Trans. Veh. Technol.*, vol. 70, no. 11, pp. 12 191–12 196, Nov. 2021.

[6] A. Bansal, K. Singh, B. Clerckx, C.-P. Li, and M.-S. Alouini, "Rate-splitting multiple access for intelligent reflecting surface aided multi-user communications," *IEEE Trans. Veh. Technol.*, vol. 70, pp. 9217–9229, Sep. 2021.

[7] B. C. Nguyen, T. M. Hoang, L. T. Dung, and T. Kim, "On performance of two-way full-duplex communication system with reconfigurable intelligent surface," *IEEE Access*, vol. 9, pp. 81 274–81 285, Jun. 2021.

[8] S. Dhok, P. Raut, P. K. Sharma, K. Singh, and C.-P. Li, "Nonlinear energy harvesting in RIS-assisted URLLC networks for industry automation," *IEEE Trans. Commun.*, vol. 69, pp. 7761–7774, Jul. 2021.

[9] A. Faisal, I. Al-Nahhal, O. A. Dobre, and T. M. N. Ngatched, "Deep reinforcement learning for optimizing RIS-assisted HD-FD wireless systems," *IEEE Commun. Lett.*, pp. 1–1, Oct. 2021.

[10] P. K. Sharma and P. Garg, "Intelligent reflecting surfaces to achieve the full-duplex wireless communication," *IEEE Commun. Lett.*, vol. 25, no. 2, pp. 622–626, Oct. 2020.

[11] A. Bansal, K. Singh, and C.-P. Li, "Analysis of hierarchical rate splitting for intelligent reflecting surfaces-aided downlink multiuser MISO communications," *IEEE Open J. Commun. Soc.*, vol. 2, pp. 785–798, Apr. 2021.

[12] W. Mei and R. Zhang, "Performance analysis and user association optimization for wireless network aided by multiple intelligent reflecting surfaces," *IEEE Trans. Commun.*, vol. 69, no. 9, pp. 6296–6312, Jun. 2021.

[13] E. Bjornson and L. Sanguinetti, "Rayleigh fading modeling and channel hardening for reconfigurable intelligent surfaces," *IEEE Wireless Commun. Lett.*, vol. 10, pp. 830–834, Apr. 2021.

[14] C. Zhang, W. Yi, Y. Liu, K. Yang, and Z. Ding, "Reconfigurable intelligent surfaces aided multi-cell NOMA networks: A stochastic geometry model," *IEEE Trans. Commun.*, pp. 1–1, Nov. 2021.

[15] Y. Cheng, K. H. Li, Y. Liu, K. C. Teh, and H. V. Poor, "Downlink and uplink intelligent reflecting surface aided networks: NOMA and OMA," *IEEE Trans. Wireless Commun.*, vol. 20, pp. 3988–4000, Feb. 2021.

[16] R. C. Ferreira, M. S. P. Facina, F. A. P. D. Figueiredo, G. Fraidenraich, and E. R. D. Lima, "Bit error probability for large intelligent surfaces under double-nakagami fading channels," *IEEE Open J. Commun. Soc.*, vol. 1, pp. 750–759, May 2020.

[17] A. Sabharwal, P. Schniter, D. Guo, D. W. Bliss, S. Rangarajan, and R. Wichman, "In-band full-duplex wireless: Challenges and opportunities," *IEEE J. Sel. Areas Commun.*, vol. 32, no. 9, pp. 1637–1652, Jun. 2014.

[18] Z. Zhang, X. Chai, K. Long, A. V. Vasilakos, and L. Hanzo, "Full duplex techniques for 5G networks: self-interference cancellation, protocol design, and relay selection," *IEEE Commun. Mag.*, vol. 53, no. 5, pp. 128–137, May 2015.

[19] E. Basar, M. Di Renzo, J. De Rosny, M. Debbah, M.-S. Alouini, and R. Zhang, "Wireless communications through reconfigurable intelligent surfaces," *IEEE Access*, vol. 7, pp. 116 753–116 773, Aug. 2019.

[20] E. Bjornson, O. Ozdogan, and E. G. Larsson, "Intelligent reflecting surface versus decode-and-forward: How large surfaces are needed to beat relaying?" *IEEE Wireless Commun. Lett.*, vol. 9, no. 2, pp. 244–248, Oct. 2020.

[21] I. S. Gradshteyn and I. M. Ryzhik, *Table of Integrals, Series, and Products*, 7th ed. San Diego, CA, USA: Academic Press, 2007.

[22] B. Zheng, C. You, and R. Zhang, "Uplink channel estimation for double-IRS assisted multi-user MIMO," in *Proc. IEEE ICC*, Montreal, QC, Canada, Jun. 2021, pp. 1–6.